# Highly Durable $Na_2V_6O_{16}·1.63H_2O$ Nanowire Cathode for Aqueous Zinc-Ion Battery

*Ping Hu,[†] Ting Zhu,[†] Xuanpeng Wang,[†] Xiujuan Wei,[†] Mengyu Yan,[§] Jiantao Li,[†] Wen Luo,[†] Wei Yang,[†] Wencui Zhang,[†] Liang Zhou,[*, †] Zhiqiang Zhou,[†] and Liqiang Mai[*, †]*

[†]State Key Laboratory of Advanced Technology for Materials Synthesis and Processing, International School of Materials Science and Engineering, Wuhan University of Technology, Wuhan 430070, China

[§]Materials Science and Engineering Department, University of Washington, Seattle, WA 98195-2120, USA

*E-mail: liangzhou@whut.edu.cn; mlq518@whut.edu.cn.

**Synthesis**

The $Na_2V_6O_{16}\cdot 1.63H_2O$ nanowires were synthesized by a hydrothermal method. In a typical synthesis, 4 mmol of $V_2O_5$ and 4 mmol of NaOH were dissolved in distilled water. The volume of the solution was set to 85 mL, and magnetically stirred at room temperature for 1h. The solution was then transferred into an autoclave and heated at 180 °C for 24 h. The sample, $Na_2V_6O_{16}\cdot 1.63H_2O$ (H-NVO) nanowire , was collected by centrifugation, washed with water and alcohol, and then dried at 80 °C overnight. The control sample, $NaV_3O_8$ (NVO) nanowire , was obtained by annealing the H-NVO nanowires at 400 °C in air for 3 h.

**Structure Characterization**

Ex situ X-ray diffraction experiments were performed on a D8 Discover X-ray diffractometer with a non-monochromated Cu Kα X-ray source. Field-emission scanning electron microscopic (FESEM) images were collected using a JSM-7001F microscope at an acceleration voltage of 10 kV. Transmission electron microscopic (TEM) and high-resolution TEM images were recorded with a JSM-2100F STEM/EDS microscope. The X-ray photoelectron (XPS) spectra were recorded on a Shimadzu Axis Ultra spectrometer with an Mg Kα = 1253.6 eV excitation source. The Brunauer-Emmett-Teller (BET) surface area was calculated from nitrogen adsorption isotherms collected at 77 K using a Tristar-3020 instrument. Thermogravimetric analysis (TGA) and differential scanning calorimeter (DSC) curves were conducted by using a Netzsch STA 449C simultaneous analyzer.

**Electrochemical Characterization**

The working electrode was fabricated by pressing a mixture of a mass ratio pf 70% active material, 20% acetylene black, and 10% polyvinylidene fluoride onto a titanium foil and dried under vacuum at 70 $^{\circ}$C for 12 h. Zn metal foil (thickness = 0.25 mm) was used as the anode, and a 3 mol $L^{-1}$ $Zn(CF_3SO_3)_2$ aqueous solution was used as the electrolyte. 2016-type coin cells were assembled by sandwiching a filter paper (Whatman grade) filled with the electrolyte between the prepared cathode and the zinc foil anode. The cyclic voltammetry (CV) test was carried out using CHI600E.

**Fabrication of H-NVO single-nanowire ZIB**

The H-NVO single-nanowire ZIB was fabricated by the following steps. Electron beam lithography (EBL) patterning of contact pads was performed on a highly doped silicon wafer with 300 nm $SiO_2$, followed by developing, rinsing, Cr/Au (5/50 nm) deposition by thermal evaporation, and then lift-off. The prepared H-NVO nanowires were then deposited on the substrate and contact pad with Cr/Au electrode through EBL patterning, developing, rinsing, Cr/Au (5/150 nm) deposition by thermal evaporation, and then lift-off. A probe station was used to check the I-V and cyclic voltammetry performances of the H-NVO nanowires. EBL patterning and developing of PMMA was used to create the isolation layer to avoid leakage current. The single-nanowire ZIB is configured with an H-NVO single-nanowire cathode, 1 M $Zn(CF_3SO_3)_2$ electrolyte, Pt counter electrode, and saturated calomel electrodes (SCE) reference electrode. The electrochemical performances of H-NVO single-nanowire ZIB was tested by An Autolab 302N Probe Station (Lake Shore, TTPX) and

Semiconductor Characterization System (B1500A).

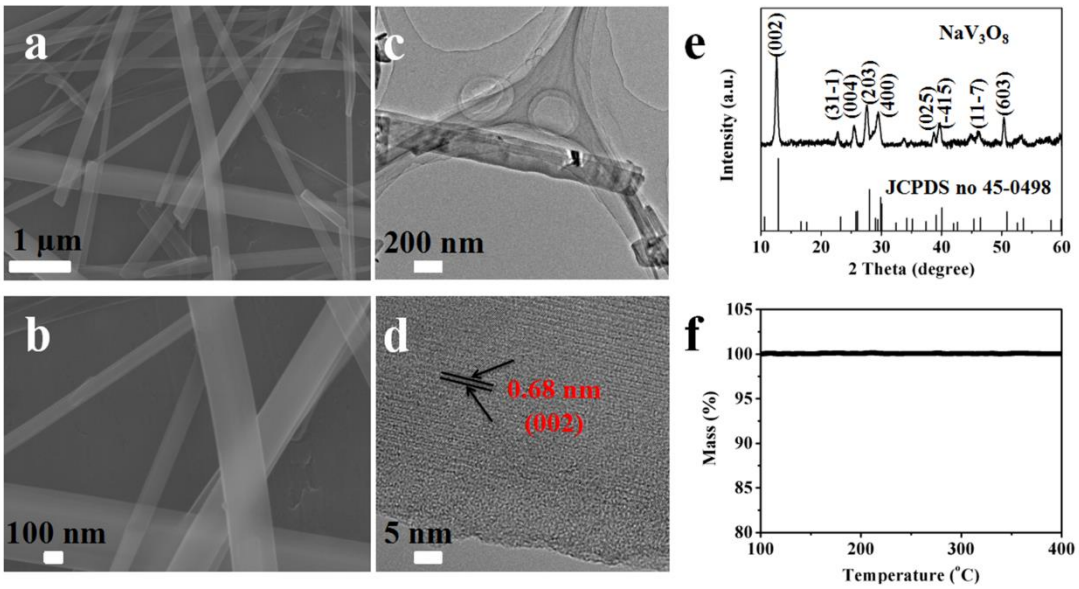


**Figure S1.** Structural characterization of NVO nanowires. SEM images (a, b), TEM images (c, d), XRD pattern (e), and TGA curve (f) of NVO nanowires.

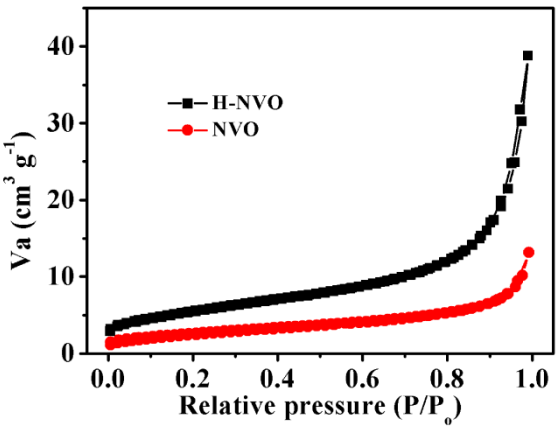


**Figure S2.** $N_2$ adsorption-desorption isotherms of H-NVO and NVO nanowires.

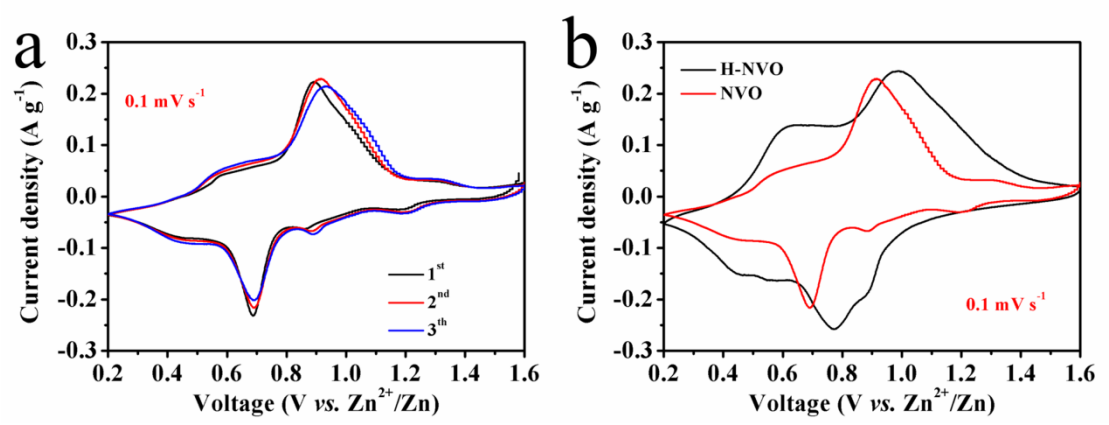


**Figure S3.** Cyclic voltammograms of NVO at a scan rate of 0.1 mV $s^{-1}$ with the electrochemical window of 0.2 – 1.6 V versus $Zn^{2+}$/Zn (a). Cyclic voltammograms of H-NVO and NVO at the scan rate of 0.1 mV $s^{-1}$ for the 2nd cycle (b).

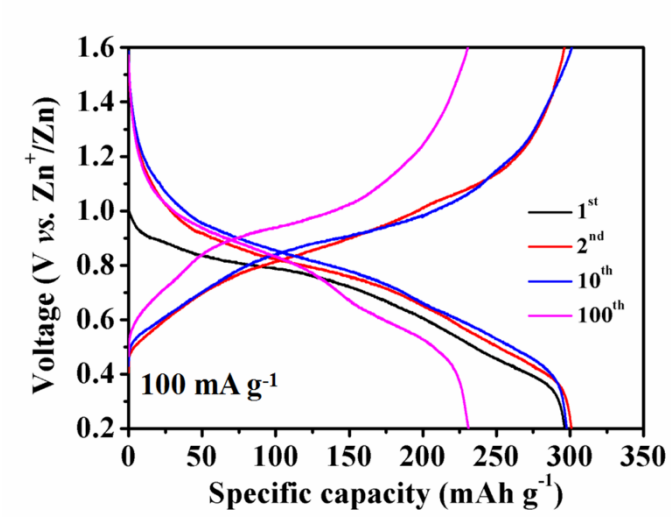

**Figure S4.** Representative charge/discharge curves of H-NVO in 3 M $Zn(CF_3SO_3)_2$ at a current density of 100 mA $g^{-1}$.

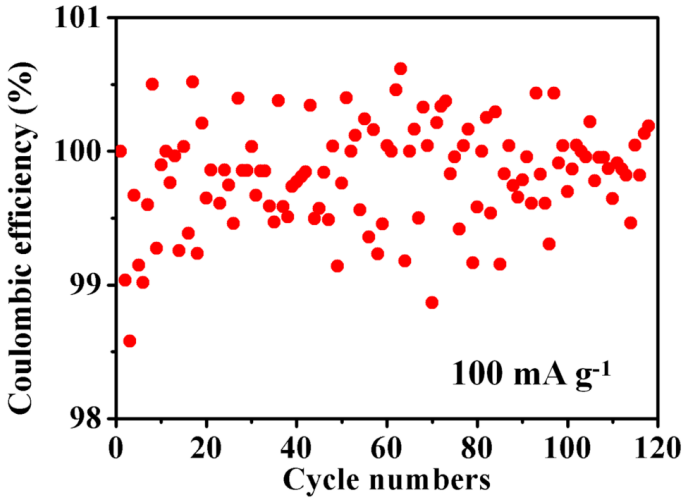


**Figure S5.** The coulombic efficiency of H-NVO in 3 M $Zn(CF_3SO_3)_2$ at a current density of 100 mA $g^{-1}$.

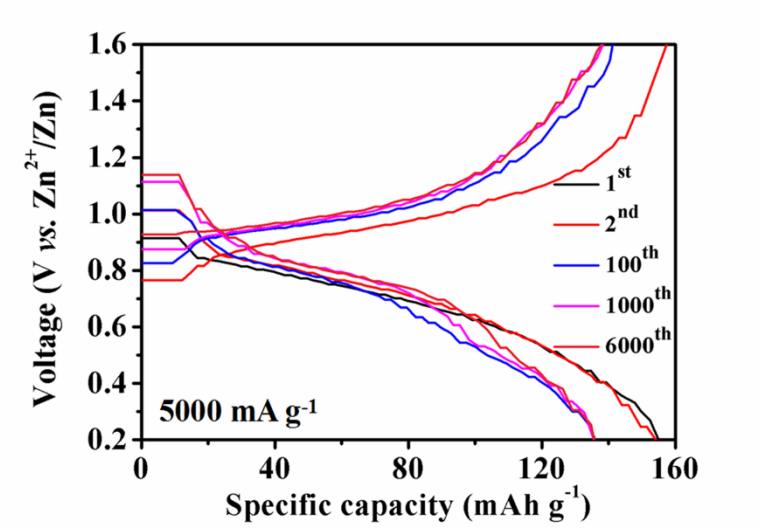


**Figure S6.** Representative charge/discharge curves of H-NVO in 3 M $Zn(CF_3SO_3)_2$ at a current density of 5000 mA $g^{-1}$.

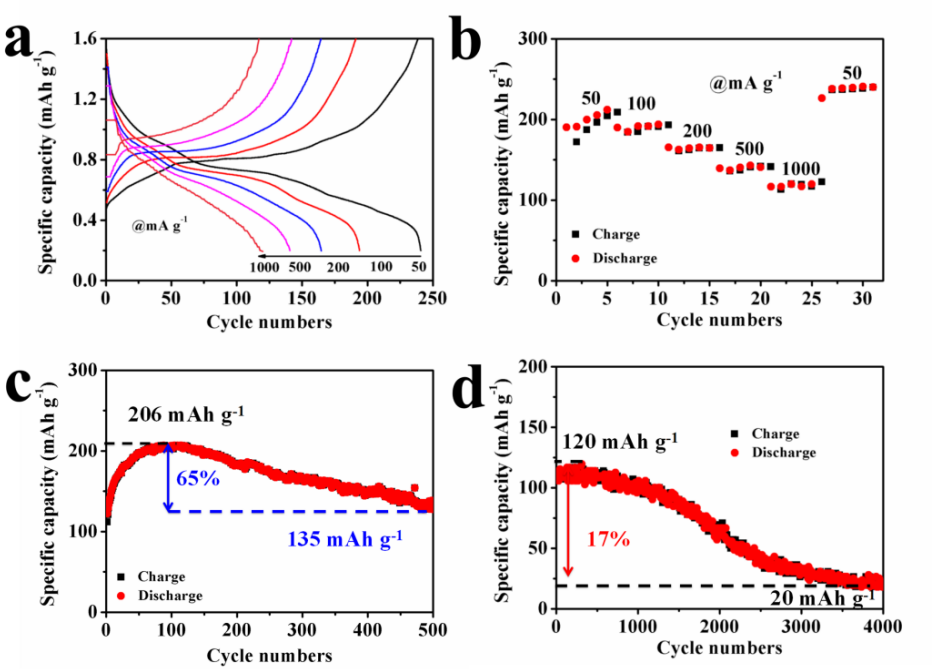


**Figure S7.** Electrochemical performances of NVO. (a) Charge/discharge curves at different current densities. (b) Rate performance of the NVO at various current densities ranging from 50 to 1000 mA $g^{-1}$. Cycling performances of the NVO at 1000 (c), and 5000 (d) mA $g^{-1}$.

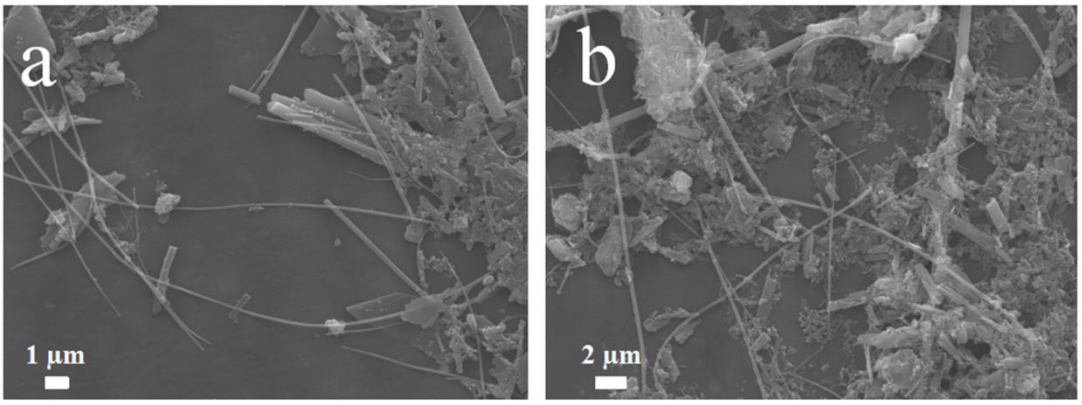


**Figure S8.** The SEM images of H-NVO after 50 cycles at 100 mA $g^{-1}$ (a) and 200 cycles at 1000 mA $g^{-1}$ (b).

**Table S1.** Electrochemical performances of recently reported vanadium-based zinc-ion battery cathode materials

| **Materials** | **Electrolyte** | **Specific capacity at *x* mA $g^{-1}$** | **Capacity retention after n cycles at y mA $g^{-1}$** | **Ref.** |
|---|---|---|---|---|
| $Na_2V_6O_{16}\cdot 1.63H_2O$ | $Zn(CF_3SO_3)_2$ | 353 (x=50) | 90% (n=6000, y=5000) | Our work |
| $Zn_{0.25}V_2O_5\cdot nH_2O$ | $ZnSO_4$ | 300 (x=50) | 80% (n=1000, y=2400) | 1 |
| $VS_2$ | $ZnSO_4$ | 190 (x=50) | 98% (n=200, y=50) | 2 |
| $LiV_3O_8$ | $ZnSO_4$ | 280 (x=16) | 75% (n=65, y=133) | 3 |
| $Na_3V_2(PO_4)_3$ | $Zn(CH_3COO)_2$ | 97 (x=50) | 74% (n=100, y=50) | 4 |
| $Na_3V_2(PO_4)_3$/C | $CH_3COONa$+ $Zn(CH_3COO)_2$ | 92 (x=50) | 74% (n=200, y=50) | 5 |
| $V_2O_5$ | AN-$Zn(TFSI)_2$ | 218 (x=14.4) | 95% (n=120, y=50) | 6 |
| $VO_{1.52}(OH)_{0.77}$ | $ZnSO_4$ | 140 (x=15) | 70% (n=50, y=15) | 7 |
| $Zn_xMo_{2.5+y}VO_{9+z}$ | $Zn(CH_3COO)_2$ | 220 (x=2) | 77% (n=30, y=2) | 8 |
| $Zn_3V_2O_7(OH)_2\cdot 2H_2O$ | $ZnSO_4$ | 213 (x=50) | 68% (n=300, y=200) | 9 |
| $H_2V_3O_8$ | $Zn(CF_3SO_3)_2$ | 423 (x=100) | 94.3% (n=1000, y=5000) | 10 |

| | | | | |
|---|---|---|---|---|
| $V_2O_5 \cdot nH_2O$ | $Zn(CF_3SO_3)_2$ | 381 (x=60) | 71% (n=900, y=6000) | 11 |

## References


1. Kundu, D. P.; Adams, B, D.; Duffort, V.; Vajargah, S. H.; Nazar, L. F. *Nature Energy* **2016**, 1, 16119.

2. He, P.; Yan, M. Y.; Zhang, G. B.; Sun, R. M.; Chen, L. N.; An, Q. Y.; Mai, L. Q. *Adv. Energy Mater.* **2017**, 7, 1601920.

3. Alfaruqi, M. H.; Mathew, V.; Song, J. J.; Kim, S. J.; Islam, S. F. Pham, D. T.; Jo, J.; Kim, S.; Baboo, J. P.; Xiu, Z. L.; Lee, K. S.; Sun, Y. K. Kim, J. *Chem. Mater.* **2017,** 29, 1684-1984.

4. Li, G. L.; Yang, Z.; Jiang, Y.; Jin, C. H. Huang, W. Ding, X. L. Huang, Y. H. *Nano Energy*, **2016**, 25, 11-217.

5. Li, G. L.; Yang, Z.; Jiang, Y.; Zhang, W. X.; Huang, Y. H. *J. Power Sources* **2016**, 308, 52-57.

6. Senguttuvan, P.; Han, S. D.; Kim, S.; Lipson, A. L.; Tepavcevic, S.; Fister, T. T.; Bloom, I. D.; Burrell, A. K.; Johnson, C. S. *Adv. Energy Mater.* **2016**, 6, 1600826.

7. Kaveevivitchai, W.; Manthiram, A. *J. Mater. Chem. A*, **2016**, 48, 18737-18741.

8. Jo, J. H.; Sun, Y. K.; Myung, S. T, *J. Mater. Chem. A*, **2017**, 5, 8367-8375.

9. Xia, C.; Guo, J.; Lei, Y. J.; Liang, H. F.; Zhao, C.; Alshareef, H. N. *Adv. Mater.*, **2017**, 1705580.

10. He, P.; Quan, Y. L.; Xu, X.; Yan, M. Y.; Yang, W.; An, Q. Y.; He, L.; Mai, L. Q. *Small*, **2017**, 1702551.

11. Yan, M. Y.; He, P.; Chen, Y.; Wang, S. Y.; Wei, Q. L.; Zhao, K. N.; Xu, X.; An, Q. Y.; Shuang, Y.; Shao, Y. Y.; Mueller, K. T.; Mai, L. Q.; Liu J.; Yang, J. H. *Adv. Mater.*, **2017**, 1703725.

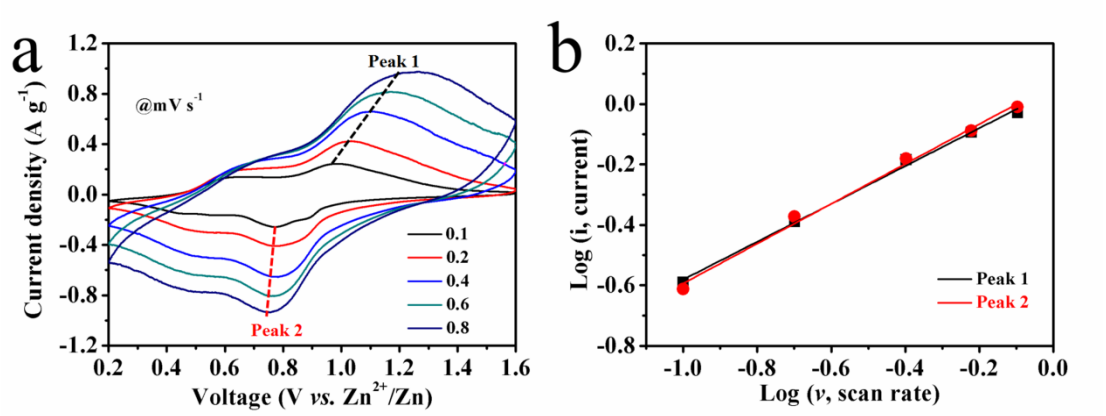


**Figure S9.** CV curves of H-NVO at different scan rates of 0.1, 0.2, 0.4, 0.6, and 0.8 mV $s^{-1}$ (a). Log(*i*) versus log(*v*) plots of the cathodic current response (b). The b-values are determined from the slopes of the fitted lines.

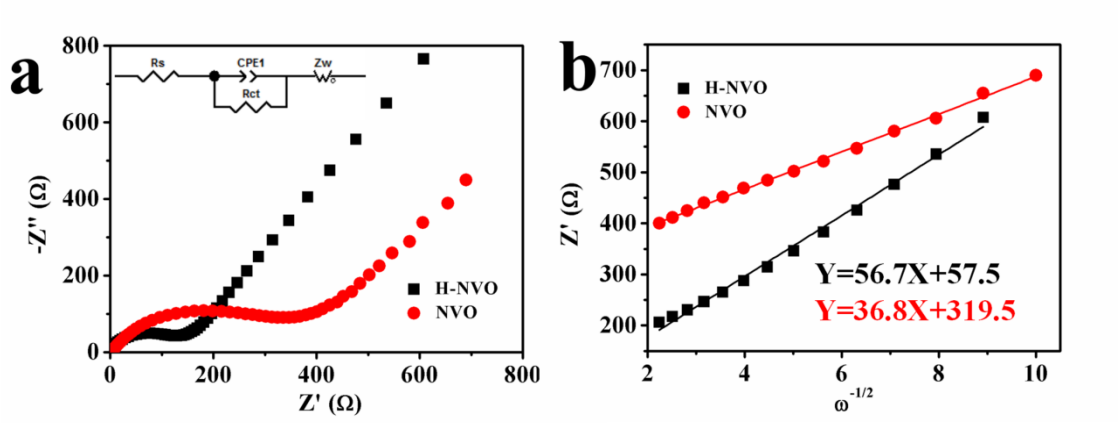


**Figure S10.** (a) Nyquist plots of H-NVO (black) and NVO (red) in 3 M $Zn(CF_3SO_3)_2$. (b) The curve of the relationship between Z' and $\omega^{1/2}$ in the low-frequency region.

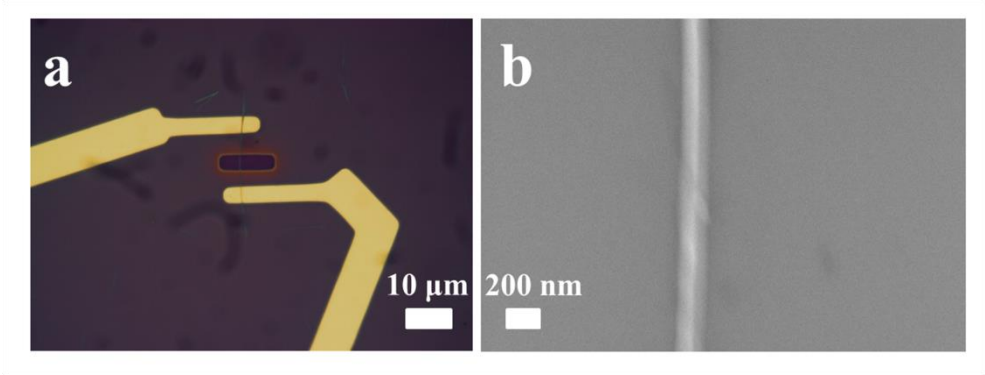


**Figure S11.** The optical image (a) and SEM image (b) of the H-NVO single-nanowire ZIB.